



3 4456 0515762 9

ORNL-4611

UC-25 - Metals, Ceramics, and Materials

cy

FABRICATION VOIDS IN ALUMINUM-BASE

FUEL DISPERSIONS

M. M. Martin

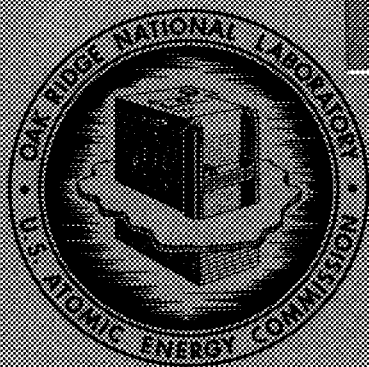
W. R. Martin

OAK RIDGE NATIONAL LABORATORY
CENTRAL RESEARCH LIBRARY
DOCUMENT COLLECTION

LIBRARY LOAN COPY

DO NOT TRANSFER TO ANOTHER PERSON

If you wish someone else to see this
document, send in name with document
and the library will arrange a loan.



OAK RIDGE NATIONAL LABORATORY

operated by

UNION CARBIDE CORPORATION

for the

U.S. ATOMIC ENERGY COMMISSION

Printed in the United States of America. Available from Clearinghouse for Federal
Scientific and Technical Information, National Bureau of Standards,
U.S. Department of Commerce, Springfield, Virginia 22151
Price: Printed Copy \$3.00; Microfiche \$9.65

LEGAL NOTICE

This report was prepared as an account of Government sponsored work. Neither the United States, nor the Commission, nor any person acting on behalf of the Commission:

- A. Makes any warranty or representation, expressed or implied, with respect to the accuracy, completeness, or usefulness of the information contained in this report, or that the use of any information, apparatus, method, or process disclosed in this report may not infringe privately owned rights; or
- B. Assumes any liabilities with respect to the use of, or for damages resulting from the use of any information, apparatus, method, or process disclosed in this report.

As used in the above, "person acting on behalf of the Commission" includes any employee or contractor of the Commission, or employee of such contractor, to the extent that such employee or contractor of the Commission, or employee of such contractor prepares, disseminates, or provides access to, any information pursuant to his employment or contract with the Commission, or his employment with such contractor.

ORNL-4611

Contract No. W-7405-eng-26

METALS AND CERAMICS DIVISION

FABRICATION VOIDS IN ALUMINUM-BASE FUEL DISPERSIONS

M. M. Martin and W. R. Martin

OCTOBER 1970

OAK RIDGE NATIONAL LABORATORY
Oak Ridge, Tennessee
operated by
UNION CARBIDE CORPORATION
for the
U.S. ATOMIC ENERGY COMMISSION

LOCKHEED MARTIN ENERGY RESEARCH LIBRARIES



3 4456 0515762 9

CONTENTS

| | <u>Page</u> |
|--|-------------|
| Abstract. | 1 |
| Introduction. | 1 |
| Description of Test Plates. | 3 |
| Characterization of Core Components | 4 |
| General Fabrication Procedures. | 7 |
| Void Volume Determination | 7 |
| Results | 10 |
| Type and Concentration of Dispersoid | 10 |
| Cladding Material. | 12 |
| Comparison Between HFIR and Miniature Plates | 14 |
| Effect of Fabrication Temperature. | 15 |
| Void Behavior During Fabrication | 16 |
| Compact Preparation | 16 |
| Hot Rolling | 19 |
| Cold Rolling and Annealing. | 20 |
| Discussion. | 21 |
| Conclusions | 23 |
| Acknowledgments | 24 |
| Appendix A. | 27 |
| Appendix B. | 31 |

FABRICATION VOIDS IN ALUMINUM-BASE FUEL DISPERSIONS

M. M. Martin and W. R. Martin

ABSTRACT

The introduction of fabrication voids explains variations in irradiation performance of many fuel dispersions for nuclear reactors. To obtain consistent and improved irradiation performance, we must understand the fabrication factors that control the amount of void volume.

The purpose of this study was to investigate the void content of aluminum-base dispersion-type fuel plates at all stages of manufacture. Two grades of U_3O_8 and two grades of UAl_x were examined at various loadings up to 1.7 g U/cm^3 of core; this covers the range applicable to the High Flux Isotope Reactor (HFIR) and the Advanced Test Reactor (ATR).

The void content of the roll-clad aluminum-base dispersions depends on (1) the type and concentration of the fuel compound, (2) the aluminum cladding alloy, and (3) the amount of cold-rolling deformation at room temperature. For a particular material combination, the first roll-bonding reduction of as little as 15% in thickness establishes a constant void concentration for all subsequent hot-rolling passes. This equilibrium quantity of voids is insensitive to the initial density of fuel compact and the amount of -325-mesh fuel particles in the dispersions. The final void content of the completed fuel plate shows only a secondary dependency on hot deformation and heat treatment.

INTRODUCTION

The control of irradiation-induced swelling in fuel dispersions by introduction of fabrication voids has been used by several investigators

to explain variations in irradiation performance.¹⁻⁴ If this concept is valid, we must understand the fabrication factors that control the final void volume in plate-type fuel elements to obtain consistent and improved irradiation performance of commercially produced fuel elements.

The purpose of this investigation is to determine and evaluate fabrication factors that affect the void concentration of aluminum-base dispersion fuel plates for research reactors. We examined two grades of U_3O_8 and two grades of UAl_x at the present uranium loadings and contemplated higher loadings of interest to the High Flux Isotope Reactor (HFIR) and Advanced Test Reactor (ATR). Standard fabrication techniques that in many instances simulated the manufacture of ATR and HFIR plates were used in preparing the experimental test plates and are discussed later in more detail.

To provide an expanded understanding of particular fabrication variables, we also made parametric studies of the effect of materials and deformation. We compared cladding alloys with various strengths, full-size HFIR plates with miniature test plates, fabrication temperatures, particle sizes of the U_3O_8 and UAl_x fuel compounds, and stages of plate processing such as pressing and degassing of the fuel compacts, individual hot and cold rolling passes, and heat treatments. The importance of each of these factors has been assessed in this report.

¹J. R. Weir, A Failure Analysis for the Low-Temperature Performance of Dispersion Fuel Elements, ORNL-2902 (May 27, 1960).

²J.D.B. Lambert, "Irradiation Study of UO_2 -Stainless Steel and $(Pu,U)O_2$ -Stainless Steel Cermet Fuels in Rod and Plate Geometry in High Temperature Nuclear Fuels," pp. 237-254 in Nuclear Metallurgy, Vol. 42, Series 12, ed. by A. N. Holden, Gordon & Breach, New York, 1968.

³M. J. Graber, M. Zukor, and G. W. Gibson, "Superior Irradiation Performance of Stainless Steel Cermet Fuel Plates Through Use of Low-Density UO_2 ," Trans. Am. Nucl. Soc. 10(2), 482-483 (November 1967).

⁴A. E. Richt, M. M. Martin, and W. R. Martin, Postirradiation Examination and Evaluation of Tungsten-Uranium Cermet, ORNL-4569 (June 1970).

DESCRIPTION OF TEST PLATES

Two types of plates were used in this investigation: a full-sized HFIR plate and a miniature irradiation test plate.

The unique HFIR plates have a tapered fuel thickness as illustrated in Fig. 1. The duplex cores for the inner and outer annulus fuel plates of the HFIR fuel element constitute a rectangular parallelepiped and consist of two mating portions: a fuel section of U_3O_8 -aluminum or UAl_x -aluminum that varies in thickness across the plate, and a filler section of aluminum. After being roll-clad with 0.0115 in. of aluminum alloy 6061, the nominal core dimensions are $20 \times 3 \times 0.027$ in. The thickness of the fuel-bearing region varies from a maximum of about 0.023 in. near the center to about 0.010 in. near the edge.

The fuel cores of our miniature plates are of uniform thickness and composition (as are the ATR fuel plates) and are roll-clad with 0.015 in.

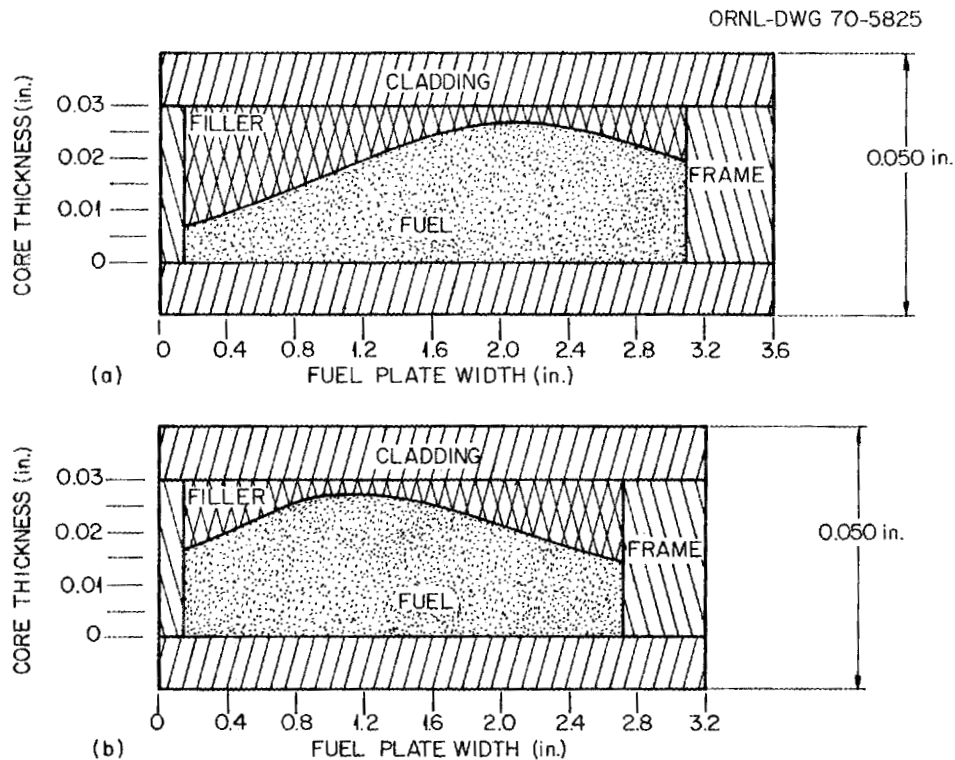


Fig. 1. Idealized Cross Sections for Experimental HFIR Fuel Plates. (a) Inner annulus. (b) Outer annulus.

of various aluminum alloys. The fuel-bearing region is nominally $5.5 \times 1 \times 0.020$ in.

Table 1 lists the range of fuel compositions fabricated for both types of fuel plates. In terms of uranium density of the fuel-bearing portion of the core, the standard outer and inner annulus loadings are, respectively, 0.85 and 1.21 g/cm³, while the standard ATR loading is 1.39. The fuel concentration range of 0.8 to 1.7 g U/cm³ of core that we examined brackets that required for HFIR and ATR fuel plates of present and contemplated higher loadings.

Table 1. Concentration Range of Dispersoids Examined

| Type of Dispersoid ^a | Concentration Range Examined | |
|--|------------------------------|--|
| | Dispersoid (wt %) | Uranium Density (g/cm ³) |
| <u>HFIR Type Plates</u> | | |
| High-fired U ₃ O ₈ | 30.2-49.8 | 0.85-1.64 |
| Burned U ₃ O ₈ | 30.6-48.7 | 0.83-1.47 |
| Solid-state-reacted UAl _x | 36.1-58.9 | 0.90-1.69 |
| <u>Miniature Plates</u> | | |
| High-fired U ₃ O ₈ | 40.2-50.2 | 1.22-1.68 |
| Burned U ₃ O ₈ | 43.8-53.0 | 1.29-1.67 |
| Solid-state-reacted UAl _x | 48.6-58.8 | 1.33-1.70 |
| Arc-cast UAl _x | 48.6-57.4 | 1.35-1.68 |

^aMaterial dispersed in Alcoa 101 aluminum.

CHARACTERIZATION OF CORE COMPONENTS

The dispersion cores were two-phase systems with particles of the uranium-bearing phase dispersed in a metallic matrix of Alcoa 101 aluminum. For the dispersed phases or fuel compounds, we examined two grades of U₃O₈ and two grades of uranium-aluminum intermetallics. Typical characteristics of the dispersoid and matrix materials are given in Table 2; actual values along with measurements of surface area and particle size

Table 2. Typical Characterization of Fuel Dispersoids and Matrix Aluminum

| Type of Material | Uranium Concentration (wt %) | Method of Fabrication | Toluene Density (g/cm ³) | Crushing Strength (g/particle) |
|---|------------------------------|--|--------------------------------------|--------------------------------|
| Atomized aluminum, Reynolds 120, Alcoa 101 | | Atomization of molten Al | 2.7 | |
| High-fired U ₃ O ₈ ^a | 84.5 | "Dead-burned" U ₃ O ₈ (Y-12 process) | 8.2 | 4 |
| Burned U ₃ O ₈ | 84.3 | Burn U metal chips | 7.6 | < 1 |
| Arc-cast UAl _x | 74.5 | Arc-cast U and Al metals | 7.0 | 42 |
| Solid-state-reacted UAl _x | 73.7 | Reaction of U hydride with Al at 1000°C | 6.7 | 108 |

^aFuel for the HFIR.

distribution measurements can be found in Appendix A for all the prepared powders used in the study.

The high-fired U_3O_8 is identical to material being successfully used⁵ in the HFIR. Its density, determined in a pycnometer with toluene, is usually greater than 98% of theoretical. Open porosity, due to sintering, is found metallographically in this material. The burned U_3O_8 is made simply by burning uranium machining chips. The burning operation is an early stage of the manufacturing process to produce high-fired U_3O_8 . The low crushing strength and density of burned U_3O_8 are less than 1 g and 7.6 g/cm^3 , respectively. These values indicate a highly friable particle containing considerable closed porosity and sometimes cracks that are inaccessible to toluene. To achieve the particular size distributions shown in Appendix A, the as-supplied high-fired and burned particles were separated into known mesh fractions and then recombined in the desired proportions. The powders were sieved up to four times to effect a stable separation.

The methods of manufacture for the uranium-aluminum intermetallics included arc-casting and hydriding techniques. Arc-cast UAl_x is a similar material to that used⁶ in the ATR. Its major crystalline constituent is UAl_3 , as determined by x-ray diffraction. The solid-state-reacted UAl_x was prepared⁷ by reacting a blend of uranium hydride and aluminum powders at 1000°C . Although both arc-cast and solid-state-reacted fuels contain UAl_2 , UAl_3 , and UAl_4 , the desired stoichiometry may be more uniformly controlled by the hydriding technique. The two grades of uranium-aluminum intermetallics thus made were crushed to powder in a dry box, sieved, and then blended in air to achieve the desired particle size distributions. In contrast to the uranium oxides, the UAl_x particles were fairly dense and had crushing strengths more

⁵W. J. Werner and J. R. Barkman, Characterization and Production of U_3O_8 for the High Flux Isotope Reactor, ORNL-4052 (April 1967).

⁶G. W. Gibson, The Development of Powdered Uranium-Aluminide Compounds for Use as Nuclear Reactor Fuels, TN-1133 (December 1967).

⁷H. J. Eding and E. M. Carr, High Purity Uranium Compounds - Final Report, ANL-6339 (1961).

than 10 times that of the two grades of U_3O_8 . Photomicrographs of the four fuels are compared in Fig. 2.

GENERAL FABRICATION PROCEDURES

The general fabrication techniques for the simulated HFIR and miniature irradiation test plates have been reported.^{8,9} The essential steps are

1. weighing and blending the component powder for each miniature fuel core and HFIR fuel and filler sections,
2. shaping the blended powders to the desired configuration in steel dies,
3. cold pressing into fuel compacts,
4. hot degassing to remove pressing lubricants and adsorbed gases,
5. assembling the degassed cores into frames and welding on cover plates to form the rolling billets,
6. cladding by hot-roll bonding,
7. annealing to soften and also to test for blistering,
8. cold rolling to a reduction in thickness of 20%,
9. heat treating to the "O" temper for aluminum, and
10. finishing operations - core location, plate shearing, cleaning, and ultrasonic nonbond inspection.

VOID VOLUME DETERMINATION

After completion of all fabrication operations, the density, D , of the core in the fabricated miniature plates was obtained from conventional pycnometer techniques described in Appendix B and the expression

$$D = \frac{W_c}{(W_a - W_s)/\rho_s - (W_a - W_c)/\rho_{Al}}, \quad (1)$$

⁸R. W. Knight, J. Binns, and G. M. Adamson, Jr., Fabrication Procedures for Manufacturing High Flux Isotope Reactor Fuel Elements, ORNL-4242 (June 1968).

⁹M. M. Martin, W. J. Werner, and C. F. Leitten, Jr., Fabrication of Aluminum-Base Irradiation Test Plates, ORNL-TM-1377 (February 1966).

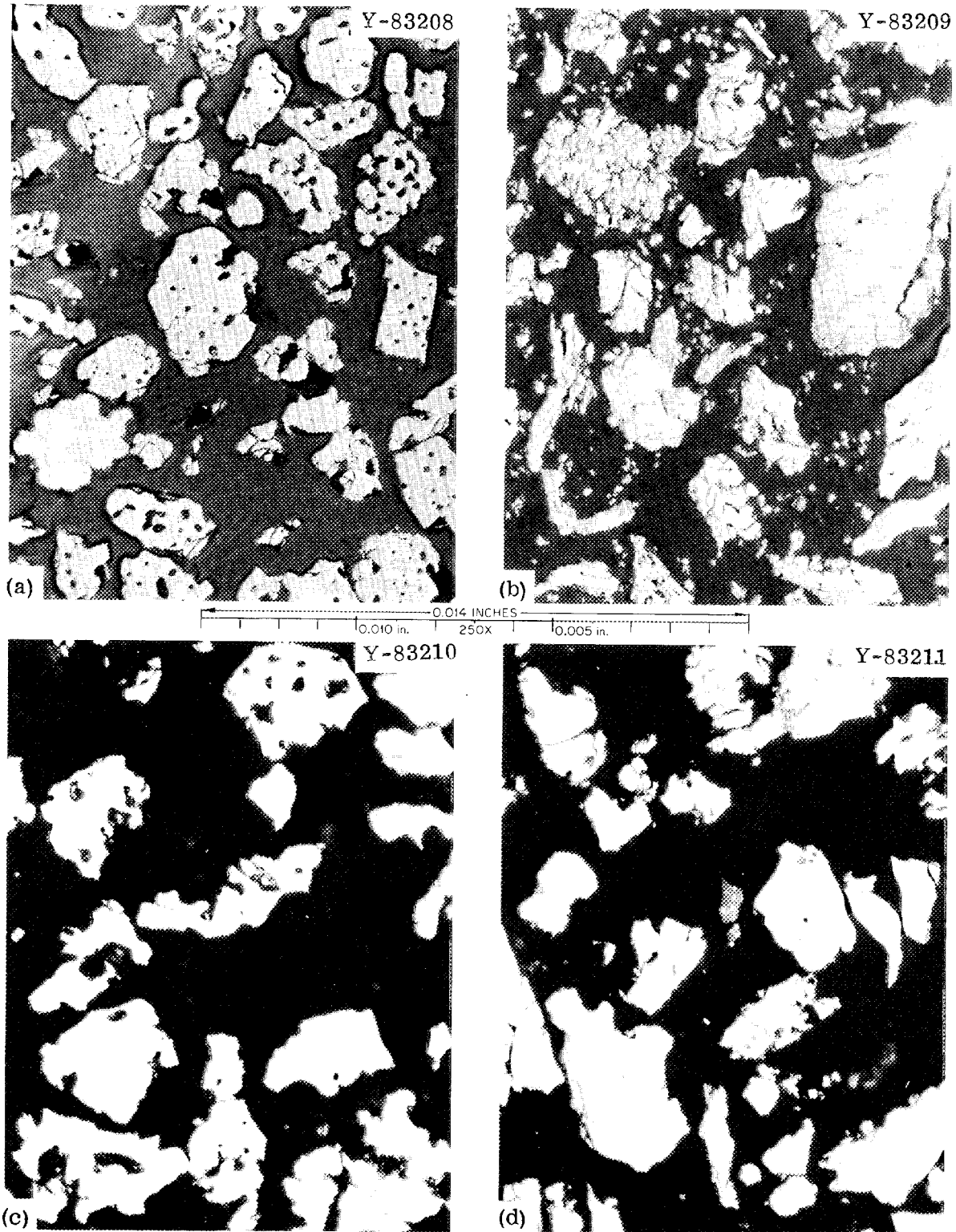


Fig. 2. Microstructures of Fuel Particles. (a) Typical "dead-burned" U_3O_8 produced at Y-12 for HFIR. (b) U_3O_8 formed by burning uranium turnings. (c) UAl_x produced by arc melting. (d) UAl_x produced by hydriding process.

where

- ρ_{Al} = density of aluminum cladding, g/cm³,
 ρ_s = density of solution, g/cm³,
 W_c = weight of core in air, g,
 W_a = weight of plate in air, g,
 W_s = weight of plate in solution, g.

For the simulated HFIR plates, we subtracted the volume of the filler section as well as the volume of the cladding. The corresponding density, DF, of the fuel bearing region is

$$DF = \frac{W_f}{(W_a - W_s)/\rho_s - (W_a - W_c)/\rho_{Al} - (W_c - W_f)/\rho_I}, \quad (2)$$

where

- ρ_I = density of the filler section, g/cm³,
 W_f = weight of the fuel section, g.

The concentration, V, of fabrication voids in the completed fuel plate was then calculated from the measured density of the fuel core and the theoretical density, ρ_t , for the dispersions:

$$V \equiv (1 - D/\rho_t) 100. \quad (3)$$

Since the UAl_x particles were not of uniform stoichiometry, we based our calculations of theoretical density for both U₃O₈ and UAl_x dispersions on the toluene density of the fuel and matrix powders. Equation (4) given below presents the usual relationship for a dispersion and serves to define theoretical density in Eq. (3).

$$\rho_t = 1/[X_f/\rho_f + (1 - X_f)/\rho_m], \quad (4)$$

where

- ρ = toluene density, g/cm³,
 X = weight fraction in uranium-bearing portion of core.

The subscripts t, f, and m denote theoretical, fuel, and matrix attributes, respectively. Please note that the definition of theoretical density effectively excludes all closed porosity within the starting fuel and

matrix powders from V of Eq. (3). In comparing irradiation results, these initial isolated voids are also important and must be considered.

RESULTS

Type and Concentration of Dispersoid

We determined the void volume of the uranium-bearing region of all the test plates for the various uranium loadings given in Table 1. The data are given in Figs. 3 and 4. In these and all like figures, the I-bars indicate the ranges of observed values for the numbers of identical plates in parentheses. The void concentrations of both types of plates exhibited excellent uniformity; the total range about the average of a group of plates was always less than ± 0.75 vol %. Regardless of

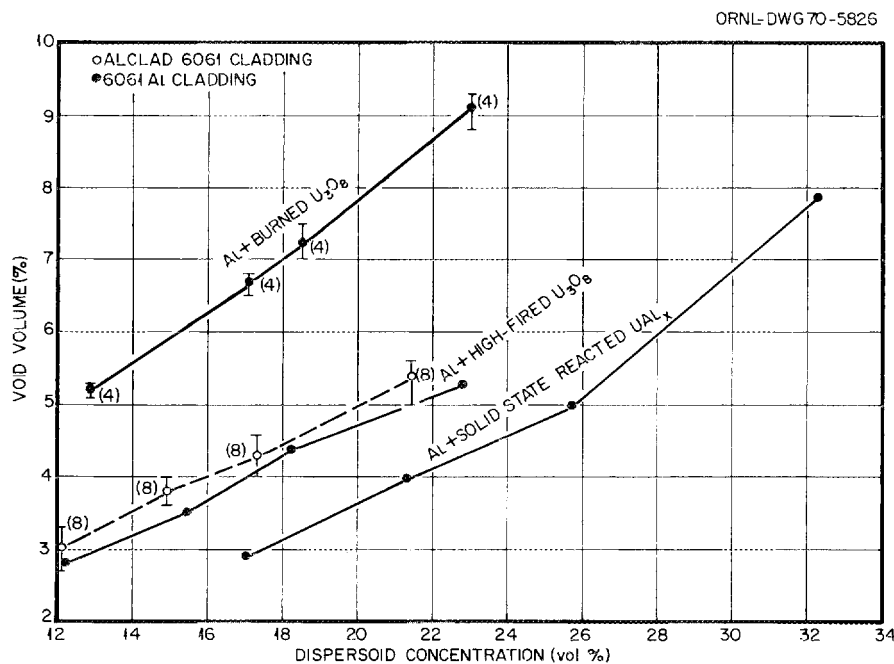


Fig. 3. Effect of Dispersoid Concentration on Void Volume of Fuel Section in Experimental HFIR Fuel Plates. Duplex fuel compacts were clad with aluminum alloys by hot rolling at 490°C . Solid and broken lines denote compacts clad respectively with 6061 and 1100-alclad 6061 aluminum alloys.

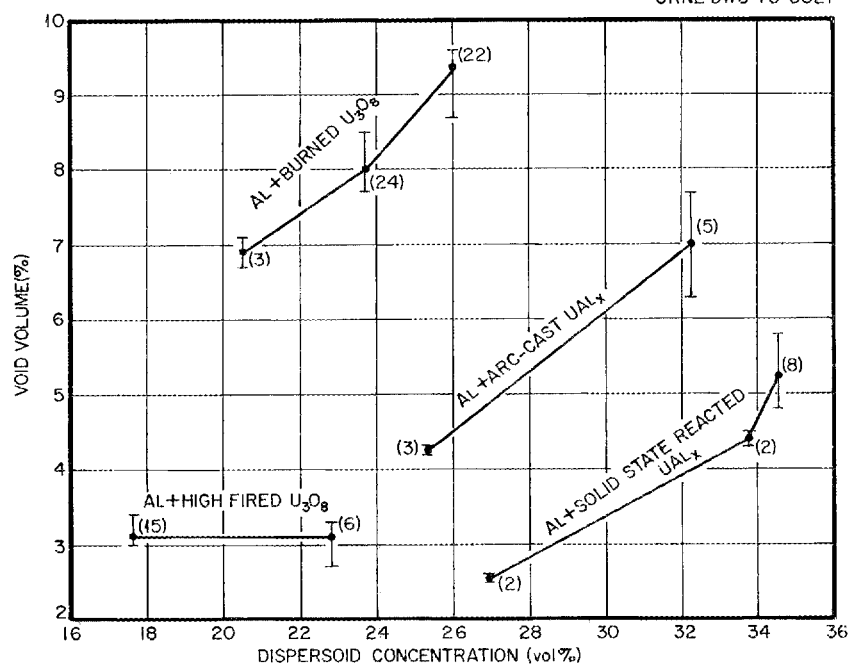


Fig. 4. Effect of Dispersoid Concentration on Core Void Volume of Miniature Test Plates. Fuel compacts were clad with 6061 aluminum alloy by hot rolling at 490°C.

the type and quantity of fuel, the HFIR and miniature plates were successfully rolled in the normal manner and without added difficulties at the higher loadings.

As depicted in Fig. 3 for HFIR plates, the void volume of the fuel section increases with fuel concentration and with the following order of fuels: solid-state-reacted UAL_x , high-fired U_3O_8 , and burned U_3O_8 . The latter order parallels the crushing strengths shown in Table 2, but our data are not sufficient to establish that a relationship between void volume and fuel crushing strength is real.

Figure 4 shows the void volume data for the miniature irradiation test plates. Although the limited concentration range covered for high-fired U_3O_8 failed to show the void volume dependency on dispersoid content, all trends cited above for the HFIR fuel sections also apply to the miniature fuel cores. For example, Fig. 4 includes data on dispersions containing arc-cast UAL_x , which has a crushing strength between that of the solid-state-reacted UAL_x and the oxides. For similar dispersoid content, these dispersions contain about 2.5 vol % more

voids than those made with the stronger fuel compound, and the burned U_3O_8 fuel exhibited more voids than either intermetallic.

Many of the points plotted in Figs. 3 and 4 represent the average void content of dispersions containing fuel compounds of various particle size distributions. Table 3 shows for identical miniature plates some

Table 3. Void Volume of Miniature Fuel Plates Containing Fuel Compounds of Various Particle Size Distributions

| Primary Particle Size Range (μm) | Fuel Fines < 44 μm (wt %) | Number of Fuel Plates | Void Volume, % | |
|--|--------------------------------------|-----------------------|----------------|---------|
| | | | Average | Range |
| <u>17.6 vol % High-Fired U_3O_8 Cores</u> | | | | |
| 44-88 | 10 | 5 | 3.3 | 3.1-3.4 |
| 44-88 | 25 | 5 | 3.0 | 3.0-3.1 |
| 44-88 | 51 | 5 | 3.1 | 3.0-3.1 |
| <u>23.6 vol % Burned U_3O_8 Cores</u> | | | | |
| 44-88 | 11 | 5 | 8.0 | 7.8-8.1 |
| 44-88 | 26 | 5 | 8.1 | 7.9-8.5 |
| 44-88 | 54 | 5 | 8.3 | 7.9-8.5 |
| <u>34.5 vol % Solid-State-Reacted UAl_x Cores</u> | | | | |
| 44-62 | 0 | 3 | 5.0 | 4.8-5.2 |
| 44-88 | 0 | 2 | 5.2 | 5.0-5.4 |
| 44-88 | 10 | 2 | 5.4 | 5.3-5.5 |
| 44-105 | 0 | 1 | 5.8 | 5.8 |

typical data that we have separated according to primary particle size range and weight percent of fuel fines. The results for solid-state-reacted UAl_x indicate that fuel fines up to 10 wt % and a particle size variation from 62 to 105 μm have little, if any, effect on the void volume. A similar statement can be made for dispersions of both burned and high-fired U_3O_8 containing up to 50 wt % fuel fines.

Cladding Material

Before we compare specifically the void volume of HFIR and miniature fuel plates, it is convenient to first consider the effect of

cladding strength. Cores of 49.4 wt % (23 vol %) burned U_3O_8 -aluminum to be rolled into miniature fuel plates were clad and framed with aluminum alloys 2219, 6061, and 1100. As one would expect, these material combinations responded differently to identical fabrication procedures. The compressive yield strength of the claddings could be related to the void concentrations in the completed fuel core, as shown in Fig. 5 for the plates clad at 500°C. We estimate¹⁰ that the compressive strength of the core was between 2500 and 3100 psi.

Void concentration and dogboning (the thickening of the core ends during rolling) follow the same trend; that is, their values are greater

¹⁰J. H. Erwin, M. M. Martin, and W. R. Martin, "The Effect of Fuel Concentration on the Compressive Strength of Core Materials Used in Research Reactor Fuel Plates," (Summary) Trans. Am. Nucl. Soc. 11(2), 490 (November 1968).

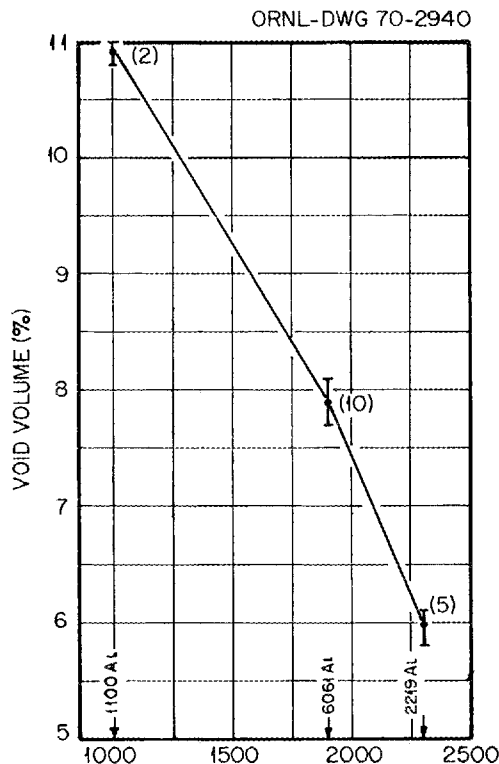


Fig. 5. Effect of Cladding Alloy on Void Volume of Miniature Plates Containing 49.4 wt % Burned U_3O_8 Cores.

when weaker cladding materials are used. Thus, replacing alloy 6061 with 2219 on a fuel plate for the ATR, for example, would probably decrease the degree of dogboning at the core ends. However, the permissible burnup level may be reduced, since less space would be available for the accommodation of irradiation-induced growth from fission products.

Comparison Between HFIR and Miniature Plates

As shown in Fig. 1, the duplex HFIR core consists of two mating portions: a fuel section containing the uranium-bearing dispersion and a filler section of aluminum. In essence, the filler material clads one side of the fuel section and in turn is bonded to the cover plate. The compressive yield strength of the filler during roll bonding at 500°C is significantly less than that of either UAl_x -aluminum or U_3O_8 -aluminum fuel sections.¹⁰ In view of the above results on cladding materials of various compressive strengths, we would therefore expect the HFIR fuel section to contain more void volume than the fuel-bearing regions of the miniature plates.

The void volume data on full-size HFIR plates are compared in Table 4 with data from the miniature plates. Our conclusion seems to

Table 4. Comparison of Void Volume in the Fuel-Bearing Region of Miniature and HFIR Fuel Plates^a

| Type of Fuel | Uranium Concentration (wt %) | Void Volume in Final Plates, vol % | |
|-----------------------------|------------------------------------|---------------------------------------|------|
| | | Miniature | HFIR |
| Solid-state-reacted UAl_x | 27 | < 1.0 | 3.2 |
| | 32 | 2.0 | 4.0 |
| | 36 | 2.5 | 4.8 |
| | 43 | 5.2 | 7.9 |
| Burned U_3O_8 | 36 | 6.3 | 7.5 |
| | 43 | 8.7 | 9.6 |

^aPlates clad with aluminum alloy 6061.

apply to fuels with both the highest and lowest crushing strengths; that is, the void volume is greater in the HFIR plate with equivalent uranium concentration. For the solid-state-reacted UAl_x , which exhibited the highest crushing strength of the fuels examined, the deviation ranged from 2.0 to 2.7 vol %. However, the difference for the very friable burned U_3O_8 was only about 1 vol %.

Effect of Fabrication Temperature

We investigated the effect of hot rolling temperature on void volume of a 23 vol % U_3O_8 dispersion clad with alloy 1100. Duplicate dispersions were roll-clad at 500, 525, 550, 575, and 600°C. Individual blends of 49.4 wt % U_3O_8 and 101 aluminum powders were first pressed at 30 tsi to 91%-dense compacts; these were then degassed for 2 hr at their designated fabrication temperatures. Degassing caused less than 2% growth in any of the pressed compacts. The treatment at 525 and 600°C produced maximum and minimum changes of 1.7 and 1.1 vol %, respectively.

After the degassing operation, duplicate compacts were hermetically sealed in 1100 aluminum alloy by roll bonding to a total reduction in thickness of 87.5% at the degassing temperature (and then 20% at room temperature). We chose core geometry and cladding thickness identical to those in our miniature plates for irradiation testing. The 1100 cladding permitted fabrication above 550°C without the eutectic melting that occurs in alloy 6061. The two final heat treatments, at the same temperature at which each compact was degassed, were for 3 and 93 hr in air.

Figure 6 presents the void volumes determined on the ten plates. Surprisingly, the above fabrication scheme did not densify the compacts processed at 500°C. In fact, the void volume retained by all of the cores of 9.9 to 10.9 vol % showed little, if any, dependency upon fabrication temperature and duration of the final anneal. Fabrication temperature in the range examined was an insignificant variable because the temperature dependency of the strength of the type 1100 alloy is very low and because the burned U_3O_8 dispersoid is compatible with the aluminum matrix.

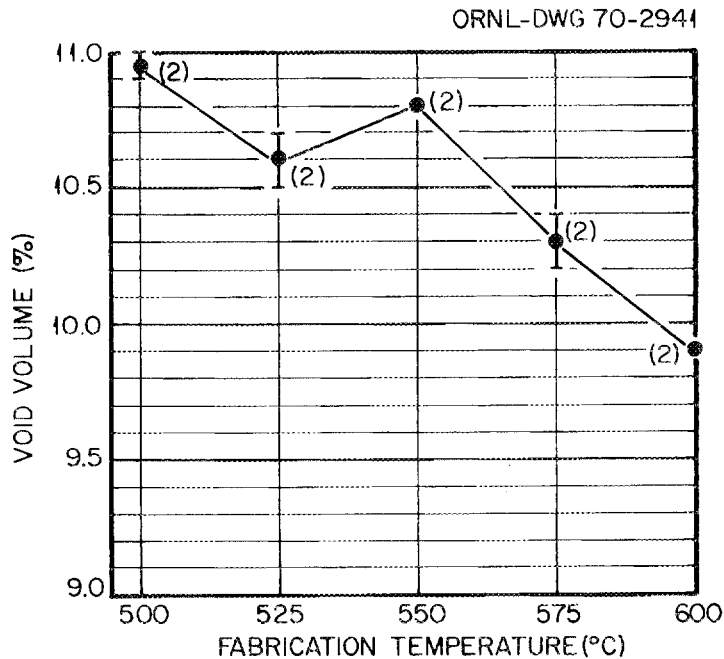


Fig. 6. Effect of Fabrication Temperature on Void Volume of Miniature Plates Containing 49.4 wt % Burned U_3O_8 in Aluminum. Fuel compacts were clad with 1100 aluminum alloy by hot rolling.

Void Behavior During Fabrication

Compact Preparation

The effect of initial compact density on the void volume of finished plates was determined for 71.6 wt % high-fired U_3O_8 and 67.2 wt % arc-cast UAl_x dispersions, which contain about 41 vol % of the fuel compound. The UAl_x loading is equivalent to the 7F element design for the ATR. For ease in fabrication we chose core geometry and cladding thickness identical to those in our miniature plates for irradiation testing.

The dispersions were fabricated as before and then clad with alloy 6061 by roll bonding at 490°C. To achieve various concentrations of voids we pressed compacts at 20, 30, and 50 tsi, and degassed some 30-tsi compacts at 400, 500, and, for the U_3O_8 -bearing compacts, 600°C.

We roll bonded four identical compacts to alloy 6061 for each of the 11 combinations of fuel compound, pressing pressure, and degassing temperature. Each group of compacts was assembled into a single rolling billet, and all were roll bonded simultaneously into four fuel plates.

Based on measurement of billet thickness at room temperature after each hot pass, their hot reductions per pass in chronological sequence averaged 15.1, 14.7, 23.5, 23.6, 24.4, 23.1, 16.7, 14.0, and about 7.3%. After hot rolling, the billets were annealed for 1 hr in air at 490°C to test for blistering. At this stage in fabrication, the total hot reduction of 83.6% yielded plates about 0.0619 in. thick.

The densities of the dispersions were determined after the pressing, degassing, and hot rolling and annealing operations. We then calculated their void contents, which are shown for the above conditions in columns 3, 4, and 5 of Table 5. In general, hot rolling and annealing decreased the void content of the prepared compacts to about 7 vol % regardless of the density after either pressing or degassing. The subsequent cold-rolling reductions increased the void content. The compacts pressed at 50 tsi are the noted exceptions to the first generalization. Surprisingly, the equilibrium void content of these hot-rolled and annealed cores is apparently slightly greater than that of the pressed compacts.

As shown in Table 5, the UAl_x -aluminum compacts pressed at 30 tsi and degassed at 500°C also deviate from the norm. These compacts consistently contained about 2 vol % more voids after the hot- and cold-rolling operations than would be expected. We note that the transformation of the UAl_x , induced by diffusion during degassing,¹¹ may have caused the large increase in the void content of the degassed compacts. Gregg *et al.*¹² demonstrated with the aid of a heating-stage metallograph that swelling of UAl_x -aluminum compacts begins with fine cracks in the fuel compound, soon followed by the growth from the cracks of a striated structure that simply forces apart the unbonded particles of the aluminum matrix. The reactions produce a heavily fragmented and brittle fuel particle. The fragmentation of the fuel particles during this reaction and also during hot rolling may have caused the additional 2 vol % void content of these compacts.

¹¹A. K. Chakraborty, R. S. Crouse, and W. R. Martin, Factors Affecting the Swelling During Degassing of Compacts Containing Uranium-Aluminum Intermetallics Dispersed in Aluminum, ORNL-TM-2800 (March 1970).

¹²J. L. Gregg, R. S. Crouse, and W. J. Werner, Swelling of UAl_3 -Al Compacts, ORNL-4056 (January 1967).

Table 5. Concentration of Voids in Dispersions of 71.6 wt % U_3O_8 and 67.2 wt % UAl_x at Various Stages of Fabrication

| Pressing Pressure (tsi) | Degassing Temperature ($^{\circ}C$) | Average Concentration of Voids, vol % | | | | | |
|---|---------------------------------------|---------------------------------------|----------|-------------------------|---------------------------|-------|----------------|
| | | Compacts | | Cores | | | |
| | | Pressed | Degassed | Hot Rolled and Annealed | Cold Reduced in Thickness | | Final Annealed |
| | | | | | 13.1% | 18.9% | |
| <u>U_3O_8-Al Dispersions</u> | | | | | | | |
| 20 | None | 13.5 | | 7.2 | 9.3 | 10.0 | 9.6 |
| 30 | None | 9.7 | | 6.7 | 9.1 | 9.8 | 9.6 |
| 50 | None | 6.7 | | 7.4 | 9.5 | 10.3 | 9.9 |
| 30 | 400 | 9.5 | 11.2 | 6.9 | 9.3 | 10.0 | 9.7 |
| 30 | 500 | 9.4 | 11.2 | 6.8 | 9.1 | 9.8 | 9.5 |
| 30 | 600 | 9.6 | 11.4 | 6.5 | 8.8 | 9.6 | 9.3 |
| <u>UAl_x-Al Dispersions</u> | | | | | | | |
| 20 | None | 13.8 | | 7.0 | 8.8 | 9.5 | 10.0 |
| 30 | None | 9.2 | | 6.8 | 8.8 | 9.5 | 9.9 |
| 50 | None | 5.8 | | 6.9 | 8.7 | 9.4 | 9.8 |
| 30 | 400 | 9.0 | 9.9 | 6.8 | 8.7 | 9.4 | 9.9 |
| 30 | 500 | 9.0 | 17.9 | 8.7 | 10.4 | 11.2 | 11.0 |

Hot Rolling

After the hot-rolling and annealing operation, we noted that the equilibrium void content of the 71.6 wt % U_3O_8 and 67.2 wt % UAl_x compacts of various initial densities was about 7 vol %. During this stage of fabrication, the compacts pressed at 20 and 30 tsi densified while those pressed at 50 tsi became slightly less dense. To elucidate when the density change occurred during hot rolling, we used the relationship

$$l_i w_i = l_0 w_0 t_0 \rho_0 / \rho_i t_i , \quad (5)$$

where l , w , t , and ρ equal, respectively, the length, width, thickness, and density of the fuel dispersion, the subscript 0 designates the initial condition of the fuel compact that is ready for billet assembly, and i designates the condition of the rolled core at any particular hot-rolling pass.

Equation (5) has the form

$$l_i w_i = A + B/t_i , \quad (6)$$

where $A = 0$ and $B = l_0 w_0 t_0 \rho_0 / \rho_i$. Thus, the slope of $l_i w_i$ plotted against $1/t_i$ should become constant if the void content reaches equilibrium during hot rolling. After each hot-rolling pass, we determined l_i and w_i from radiographs of the rolled billet and also measured the billet thickness T_i . By assuming that the core thickness reduced proportionately to the billet reduction, t_i was estimated according to

$$t_i = \hat{t}_i = t_0 T_i / T_0 , \quad (7)$$

where \hat{t}_i represents the calculated core thickness for a particular pass, i .

For each of the dispersions characterized previously in Table 5, we calculated by the method of least squares the intercept A , the slope B , and the root-mean-square, S_y , of the $l_i w_i$ deviations for Eq. (6). The correlation was made for hot-rolling passes 1 through 8. As shown in Table 6, the standard error of estimate, S_y , is effectively zero and indicates that an excellent fit of the data to the linear equation was

Table 6. Least-Squares Fit of $l_i w_i = A + B/t_i$ for Hot-Rolled 41 vol % U_3O_8 and UAl_x Fuel Dispersions

| Pressing Pressure (tsi) | Degassing Temperature ($^{\circ}C$) | Intercept A ($in.^2$) | Slope B ($in.^3$) | Standard Error of Estimate ($in.^3$) |
|---|---------------------------------------|-------------------------|---------------------|--|
| <u>U_3O_8-Al Dispersions</u> | | | | |
| 20 | None | 0.052 | 0.101 | 0.015 |
| 30 | None | 0.055 | 0.102 | 0.011 |
| 50 | None | 0.070 | 0.102 | 0.010 |
| 30 | 400 | 0.062 | 0.102 | 0.007 |
| 30 | 500 | 0.058 | 0.102 | 0.005 |
| 30 | 600 | 0.061 | 0.102 | 0.006 |
| <u>UAl_x-Al Dispersions</u> | | | | |
| 20 | None | 0.068 | 0.100 | 0.000 |
| 30 | None | 0.071 | 0.100 | 0.007 |
| 50 | None | 0.066 | 0.102 | 0.008 |
| 30 | 400 | 0.062 | 0.100 | 0.006 |
| 30 | 500 | 0.089 | 0.101 | 0.010 |

obtained. The intercept is also near zero, as predicted from Eq. (5). The slope of about 0.102 in.^3 is constant for the two types of dispersions with various initial densities. If pass 1 is excluded from the correlation, the slopes remain 0.102 in.^3 . We conclude that both the U_3O_8 - and UAl_x -aluminum cores achieved their equilibrium void content on the first rolling pass. Further hot rolling, at least through 83.6% reduction in thickness, elongates and widens the core without changing its density.

Cold Rolling and Annealing

To investigate the effect of cold rolling, we continued the fabrication of the miniature plates containing about 41 vol % of dispersoid. After hot rolling and annealing, they were reduced 18.9% in thickness at room temperature by four rolling passes at each of the six mill settings 0.059, 0.057, 0.055, 0.053, 0.051, and 0.050 in. To complete their fabrication, we annealed the cold-rolled plates 3 hr at $490^{\circ}C$ and then slowly cooled them to produce the "0" temper in the 6061 aluminum alloy cladding.

During cold rolling, both the oxide and intermetallic fuel phases fragment and form stringers. One would, therefore, expect void volume of dispersion fuels to increase with deformation at room temperature. The high-fired U_3O_8 compound, however, appears to form a more friable particle than does arc-cast UAl_x . In Table 5, the column "Cold Reduced in Thickness 13.1%" lists the void content of the fuel dispersions after a reduction in thickness of 13.1% at room temperature. This degree of working increased the void content about 2.3 and 1.8 vol % for the U_3O_8 - and UAl_x -bearing cores, respectively. Further cold rolling to a total reduction of 18.9% produced an additional linear increase of about 0.7 vol % voids for both types of dispersions.

The final annealing operation affects the void contents of the two types of dispersions differently. A comparison of the values for cold-rolled and final-annealed materials in Table 5 for the U_3O_8 -aluminum cores shows an average decrease of 0.3 vol %. A similar change of 0.2 vol % can be noted for the UAl_x -aluminum cores pressed at 30 tsi and degassed at 500°C. We believe that this slight reduction in average void concentration denotes sintering of the cold-rolled materials. For the UAl_x -aluminum cores, it also implies that the reaction between the UAl_x fuel particles and the aluminum matrix is now complete. However, this is not so for the remaining UAl_x -aluminum cores pressed at 20, 30, or 50 tsi or for those pressed at 30 tsi and degassed at 400°C. These clad dispersions increased about 0.4 vol % in average void content, probably from the transformation of UAl_x during the final heat treatment.

DISCUSSION

We analyzed the results to determine and evaluate those fabrication factors that control the concentration of voids during fuel plate manufacture. A generalized treatment of the data, showing the effect of deformation on the void content of dispersion fuel plates, will perhaps serve to present and summarize our findings. For example, consider two aluminum-base dispersions, a and b. These may contain either two types of fuel compounds or the same fuel compound of differing dispersoid concentration.

Figure 7 schematically illustrates the effect of deformation on a- and b-type dispersions at the various stages of fabrication into composite plates. The symbols a^V and b^V denote the void concentration of the a and b dispersions, respectively. Superscripts affixed to either a^V or b^V identify a particular stage of fabrication (D = pressing and/or degassing, HD = hot deformation, BA = blister anneal, CD = cold deformation, and F = final heat treatment). Our illustration starts with four vertically plotted points (a^{VD_1} , a^{VD_2} , b^{VD_1} , b^{VD_2}) that represent the relative void levels of a and b dispersions after pressing at (1) 50 tsi and (2) 20 tsi. We note that V^D depends on the type and concentration of the dispersoid, the pressing pressure, and the heat treating temperature used to degas the compacts before rolling.

As depicted in Fig. 7, we found that V^{HD} may be either less than, equal to, or greater than V^D , depending on the pressing and degassing

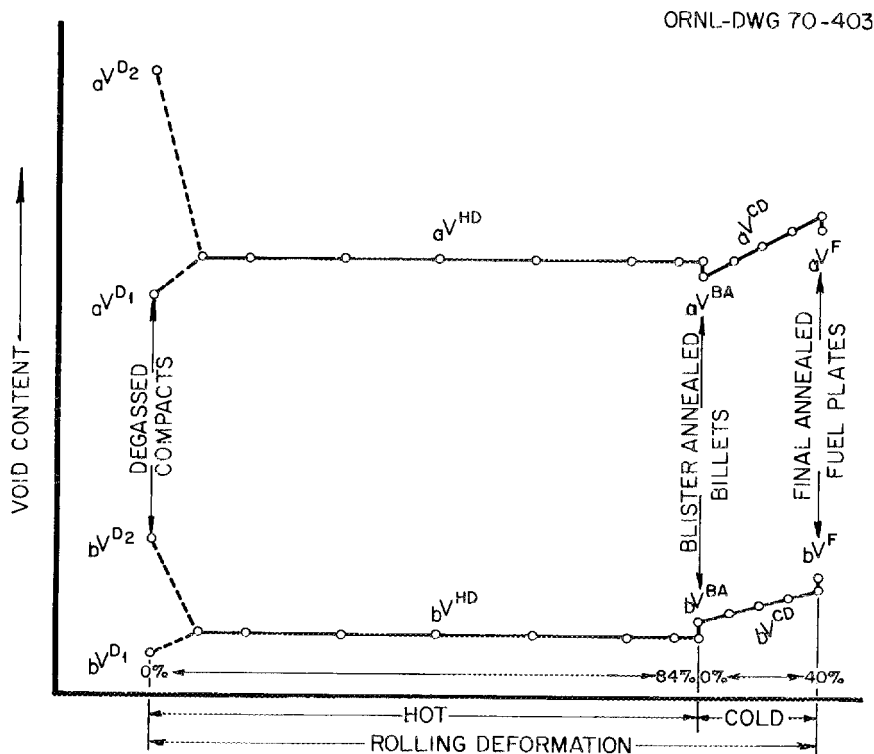


Fig. 7. Schematic Illustration of the Effect of Deformation on the Void Contents, a and b, of Two General Aluminum-Base Dispersions.

conditions for the powder-metallurgy compacts. It remains constant during all hot-rolling passes. In dispersions that are composed of chemically compatible materials, V^{HD} is also independent of V^D . The blister annealing treatment given the plates after hot rolling produces little change from V^{HD} . However, V^{BA} can be either less than, equal to, or greater than V^{HD} . In Fig. 7, aV^{BA} depicts a slight degree of sintering with respect to aV^{HD} , while bV^{BA} shows an increase we postulated because of a reaction between the dispersoid and aluminum matrix.

Cold rolling increases the void content of dispersion-type fuels but the amount of the change depends on the type and probably the concentration of the dispersoid. The slope shown in Fig. 7 for V^{CD} represents a linear increase of 0.1 to 0.2% void volume per 1% deformation at room temperature. That rate was shown by dispersions of high-fired U_3O_8 and arc-cast UAl_x containing about 41 vol % of the fuel compound. This observation presents the fabricator with an easy way to increase the void content of dispersion fuel plates. The final void content of the dispersion, V^F , shows only a secondary dependency on deformation and heat treatment but depends principally on the type and concentration of the dispersions. However, one must recognize that the secondary influence of deformation and heat treatment on void volume could significantly influence the irradiation performance of dispersion plates.

CONCLUSIONS

The results of the investigations on fabrication voids in aluminum-base dispersion fuel plates indicate the following:

1. The type and concentration of the fuel compounds affect the void content of the clad fuel dispersion. The quantity of voids increases with increasing concentration and apparently with decreasing crushing strength of the fuel compounds.
2. The type of aluminum alloy cladding affects the void content of the clad fuel dispersions. The quantity of voids is greater for cladding materials of lower compressive yield strength.
3. Only 15% reduction in thickness at 500°C to the dispersions establishes a constant void concentration for all subsequent hot-rolling

passes. This equilibrium void volume is independent of compact pressing pressure and also compact degassing temperature if the dispersion is composed of chemically compatible materials.

4. Deformation at room temperature increases the void content of the clad dispersions.

ACKNOWLEDGMENTS

The assistance rendered by various members of the Metals and Ceramics Division is gratefully acknowledged. Special acknowledgment is given to L. L. Allen, W. R. Johnson, H. E. Reesor, and H. J. Wallace, who manufactured the test plates. The rolling operation was directed by J. H. Erwin.

APPENDIX A

Appendix A

Characterization of Fuel Dispersoids and Matrix Aluminum

| Type of Material | Powder Blend Designation | Uranium Content, wt % | | Particle Size ^a | | Crushing Strength (g) | Surface Area ^b (m ² /g) | Toluene Density (g/cm ³) |
|--------------------------------------|--------------------------|--|------------------|----------------------------|-------------------------|-----------------------|---|--------------------------------------|
| | | Total | ²³⁵ U | Principal Range (μm) | Fines of < 44 μm (wt %) | | | |
| | | High-Fired U ₃ O ₈ | DHFA | 84.8 | 0.2 | | | |
| | HFAC ^c | 84.7 | 93.2 | 44-88 | 3 | | 0.04 | 8.22 |
| | PB-1 ^c | 84.5 | 93.2 | 44-88 | 10 | ~ 4 | 0.05 | 8.22 |
| | PB-2 ^c | 84.2 | 93.2 | 44-88 | 25 | | 0.06 | 8.25 |
| | PB-3 ^c | 84.5 | 93.2 | 44-88 | 51 | | 0.07 | 8.26 |
| | A | 84.7 | 93.2 | 44-88 | 9 | | 0.05 | 8.24 |
| | B | 84.7 | 93.2 | 74-88 | 0 | | 0.05 | 8.22 |
| | C | 84.5 | 93.2 | 44-88 | 2 | | 0.05 | 8.22 |
| | D | 84.8 | 93.2 | 0-44 | 100 | | 0.06 | 8.25 |
| Burned U ₃ O ₈ | FA ^c | 84.5 | 93.2 | 44-105 | 3 | | 0.35 | 7.60 |
| | PB-4 ^c | 84.3 | 93.2 | 44-88 | 11 | < 1 | 0.34 | 7.64 |
| | PB-5 ^c | 84.4 | 93.2 | 44-88 | 26 | | 0.38 | 7.65 |
| | PB-6 ^c | 84.1 | 93.2 | 44-88 | 54 | | 0.35 | 7.65 |
| | PB-7 | 84.5 | 93.2 | 44-88 | 2 | | 0.34 | 7.58 |
| Solid-State-Reacted UAl _x | DH | 73.9 | 0.2 | 44-88 | 27 | | 0.09 | 6.87 |
| | HA ^c | 73.7 | 93.2 | 88-105 | 0 | 108 | 0.08 | 6.70 |
| | HB ^c | 73.7 | 93.2 | 53-88 | 0 | | | |
| | HC ^c | 73.7 | 93.2 | 44-53 | 0 | | 0.10 | 6.70 |
| | HD ^c | 73.7 | 93.2 | 44-88 | 10 | | | |
| Arc-Cast UAl _x | AA ^c | 75.2 | 93.2 | 44-88 | 10 | 42 | 0.11 | 7.10 |
| Atomized Aluminum | A-101 | | | 44-105 | 90 | | 0.22 | 2.70 |

^aStandard sieve analysis.

^bStatic BET krypton or nitrogen surface area.

^cThese materials were subsequently irradiated.

APPENDIX B

Appendix B

Density Determination

Equipment:

Analytical balance (precision = ± 0.001 g) modified for weighing
below pan
Stainless steel wire
Cylindrical Pyrex container
Distilled water, ($\geq 500,000$ ohm)
Kodak Photo-Flow 200
Clean lint-free gloves
Clean soft lint-free cloth
Acetone
Plate holder
Thermometer, graduated to 0.1°C

Procedure:

1. Receive batch of pickled fuel plates.
2. Examine plate surfaces for finger prints, oil, foreign material, and dirt. If contamination is noted, thoroughly wipe plate surfaces with acetone using clean soft lint-free cloth. Allow surface to air dry for 5 min.
3. Weigh plates in air to nearest 0.001 g.
 - (a) Zero balance with wire in place.
 - (b) With balance fully arrested, gently hang plate in air beneath pan.
 - (c) Weigh plate. Record weight after balance comes to rest.
 - (d) With balance fully arrested, remove plate and place in holder.
 - (e) Repeat for all plates in batch.
4. Weigh plates in water to nearest 0.001 g.
 - (a) Place cylindrical Pyrex container containing solution beneath balance.
 - (b) Zero balance with wire hanging in solution.

- (c) Using wire, submerge and gently agitate plate in solution to remove air bubbles.
- (d) Without exposing plate surface to air and with the balance fully arrested, hang plate in solution beneath pan.
- (e) Weigh plate. Record weight after balance comes to rest.
- (f) Record temperature of solution to nearest 0.1°C.
- (g) With balance fully arrested, remove and wipe plate with clean soft lint-free cloth. Place dry plate in holder.
- (h) Repeat for all plates in batch.

General:

1. Analytical balance is to be calibrated against NBS standardized weights before each use.
2. Solution contains 1 ml Kodak Photo-Flow 200 per gallon of distilled water.
3. Handle plates only with clean lint-free gloves.
4. Before weighing, plates, balance, and solution must be at the same temperature.

ORNL-4611
UC-25 - Metals, Ceramics, and Materials

INTERNAL DISTRIBUTION

- | | | | |
|--------|-------------------------------|--------|-------------------------------|
| 1-3. | Central Research Library | 44. | E. L. Long, Jr. |
| 4. | ORNL - Y-12 Technical Library | 45. | A. L. Lotts |
| | Document Reference Section | 46-50. | M. M. Martin |
| 5-24. | Laboratory Records Department | 51-55. | W. R. Martin |
| 25. | Laboratory Records, ORNL RC | 56. | R. W. McClung |
| 26. | ORNL Patent Office | 57. | R. V. McCord |
| 27. | G. M. Adamson, Jr. | 58. | H. E. McCoy, Jr. |
| 28. | R. J. Beaver | 59. | C. J. McHargue |
| 29. | J. V. Cathcart | 60. | P. Patriarca |
| 30. | G. L. Copeland | 61. | A. E. Richt |
| 31. | J. A. Cox | 62. | G. M. Slaughter |
| 32. | F. L. Culler | 63. | J. O. Stiegler |
| 33. | J. E. Cunningham | 64. | D. A. Sundberg |
| 34. | R. G. Donnelly | 65. | D. B. Trauger |
| 35. | J. H. Erwin | 66. | A. M. Weinberg |
| 36. | J. H. Frye, Jr. | 67. | J. R. Weir |
| 37. | J. C. Griess, Jr. | 68. | C. M. Adams, Jr. (Consultant) |
| 38. | W. O. Harms | 69. | Leo Brewer (Consultant) |
| 39. | R. F. Hibbs | 70. | L. S. Darken (Consultant) |
| 40-42. | M. R. Hill | 71. | Walter Kohn (Consultant) |
| 43. | R. W. Knight | | |

EXTERNAL DISTRIBUTION

72. F. W. Albaugh, Battelle-Northwest
73. F. H. Anderson, Idaho Nuclear Corp., P.O. Box 1845, Idaho Falls, Idaho 83401
74. D. Baily, AEC, Washington
75. R. D. Baker, Los Alamos Scientific Laboratory
76. B. J. Beers, Idaho Operations Office, USAEC, Idaho Falls, Idaho 83401
77. W. C. Bills, Idaho Operations Office, USAEC, Idaho Falls, Idaho 83401
78. D. F. Cope, RDT, SSR, AEC, Oak Ridge National Laboratory
79. J. W. Crawford, AEC, Washington
80. D. R. deBoisblanc, Idaho Nuclear Corp., P.O. Box 1845, Idaho Falls, Idaho 83401
81. N. J. Donahue, AEC, Savannah River Operations
82. W. C. Francis, Idaho Nuclear Corp., P.O. Box 1845, Idaho Falls, Idaho 83401
83. A. Giambusso, AEC, Washington
84. G. W. Gibson, Idaho Nuclear Corp., P.O. Box 1845, Idaho Falls, Idaho 83401

85. M. J. Graber, Idaho Nuclear Corp., P.O. Box 1845,
Idaho Falls, Idaho 83401
86. J. Griffith, Idaho Operations Office, USAEC, Idaho Falls,
Idaho 83401
87. D. H. Gurinsky, Brookhaven National Laboratory
88. E. E. Hayes, DuPont, Wilmington
89. R. T. Jones, AEC, Washington
90. E. E. Kintner, AEC, Washington
91. S. R. Knight, Idaho Nuclear Corp., P.O. Box 1845,
Idaho Falls, Idaho 83401
92. V. M. Kolba, Argonne National Laboratory
93. M. Levenson, Argonne National Laboratory
94. J. L. Liebenthal, Idaho Nuclear Corp., P.O. Box 1845,
Idaho Falls, Idaho 83401
95. C. L. Matthews, RD1, OSR, AEC, Oak Ridge National Laboratory
96. M. Nevitt, Argonne National Laboratory
97. G. Norman, AEC, Washington
98. P. H. Permar, Savannah River Laboratory
99. J. B. Phillipson, Idaho Nuclear Corp., P.O. Box 1845,
Idaho Falls, Idaho 83401
100. W. O. Rathbun, AEC, Richland
101. D. Rauch, AEC, Washington
102. W.L.R. Rice, AGMR, AEC, Washington
103. M. A. Rosen, AEC, Washington
104. H. M. Roth, AEC, Oak Ridge Operations
105. L. S. Rubenstein, AEC, Washington
106. J. M. Simmons, Division of Reactor Development and Technology,
AEC, Washington
107. D. K. Stevens, Division of Research, AEC, Washington
108. E. F. Sturcken, Savannah River Laboratory
109. F. H. Tingey, Idaho Nuclear Corp., P.O. Box 1845, Idaho Falls,
Idaho 83401
110. G. Tuer, Savannah River Laboratory
111. A. Van Echo, AEC, Washington
112. W. R. Voight, Jr., AEC, Washington
113. V. Wahler, AEC, Washington
114. W. W. Ward, AEC, Washington
115. C. E. Weber, AEC, Washington
116. L. J. Weber, Idaho Nuclear Corp., P.O. Box 1845, Idaho Falls,
Idaho 83401
117. M. C. Whittels, Division of Research, AEC, Washington
118. R. E. Wood, Idaho Operations Office, USAEC, Idaho Falls,
Idaho 83401
119. Laboratory and University Division, AEC, Oak Ridge Operations
120. Patent Office, AEC, Oak Ridge Operations
- 121-319. Given distribution as shown in TID-4500 under Metals, Ceramics,
and Materials category (25 copies - CFSTI)